18. B. M. Crowe, *Am. Nucl. Soc. Proc. High-Level Rad. Waste Manage. Conf.* **1**, 65 (1990).
19. D. T. Vaniman, B. M. Crowe, E. S. Gladney, *Contrib. Mineral. Petrol.* **80**, 341 (1982).
20. All samples were collected as cores with a portable drill and nonmagnetic drill bits. Sample azimuths were obtained with the use of solar compass readings. Samples were cut into standard 2.5 cm by 2.2 cm right-cylinder specimens
21. A three-axis superconducting rock magnetometer (2G Enterprises Model 760R) was used for all remanence measurements. Progressive alternating field and thermal demagnetization was done with commercial 2G Enterprises and Schonstedt instruments, respectively.
22. C. D. Ratcliff, thesis, University of New Mexico, Albuquerque (1993); C. D. Ratcliff, J. W. Geissman, F. Perry, in preparation.
23. We used principal component analysis on discrete trajectories to determine the direction of the best-fit line; lines (always unanchored) with maximum angular deviations greater than 15° were rejected. Where two discrete components of magnetization, one with unblocking temperatures greater than 580°C carried by hematite, were identified in demagnetization diagrams, we always used the magnetite-dominated magnetization isolated below 580°C as that characteristic of the site. Site means were determined by calculating the Fisherian mean of characteristic linear segments from accepted, individual samples. At least 60% of the samples from each site were used in the determination, and site means with α_{95}'s (*28*) greater than 15° were rejected.
24. Isothermal remanent magnetization acquisition experiments show essentially complete saturation by 150 to 250 mT. Hysteresis data from fresh, fine-grained intrusions show that these rocks are characterized by coercivities between 18 and 26 mT, ratios of saturation remanence to saturation magnetization between 0.17 and 0.24, and ratios of coercivity of remanence to coercivity between 2.2 and 2.9, consistent with abundant fine magnetite as the principal remanence carrier.
25. N. D. Watkins, *Geotimes* **4**, 18 (1976).
26. C. W. F. Everitt and J. A. Clegg, *Geophys. J. R. Astron. Soc.* **6**, 312 (1962). Paleomagnetic contact tests are considered positive if, at high statistical confidence, both the intrusion and adjacent host rock have essentially the same remanence direction, yet more distant host rocks retain a distinct preintrusion remanence. Because the magnetic mineralogy usually differs from that of the remagnetized host, agreement of ChRMs in a contact test suggests a primary magnetization for the intrusion.
27. Host ash-flow tuffs and associated deposits in the Paiute Ridge area are poorly welded or poorly indurated, or both. It was difficult to sample these rocks where they had not been baked by the intrusions.
28. [illegible] the cone of 95% [illegible] ean direction; *k* is the concentration parameter.
29. P. L. McFadden and F. Lowes, *Geophys. J. R. Astron. Soc.* **67**, 19 (1981).
30. R. S. Coe and M. Prevot, *Earth Planet. Sci. Lett.* **92**, 292 (1989).
31. A. Stephenson, S. Sadikun, D. K. Potter, *Geophys. J. R. Astron. Soc.* **84**, 185 (1986).
32. R. B. Hargraves, D. Johnson, C. Y. Chan, *Geophys. Res. Lett.* **18**, 2193 (1991).
33. W. J. Carr, *Geol. Soc. Am. Mem.* **176**, 283 (1990).
34. M. R. Hudson, *Geol. Soc. Am. Bull.* **104**, 581 (1992).
35. J. G. Rosenbaum, M. R. Hudson, R. B. Scott, *J. Geophys. Res.* **96**, 1963 (1991).
36. M. R., Hudson, D. A. Sawyer, R. G. Warren, *Tectonics* **13**, 258 (1994).
37. A whole-rock K-Ar age of 8.5 ± 0.3 Ma was reported by B. M. Crowe, S. Self, D. Vaniman, R. Amos, and F. Perry [*J. Geol.* **91**, 259 (1983)]. For our determinations, samples from three sites include sanidine from a fused ash-flow tuff from within 1 m of the upper contact with the Paiute Ridge lopolith, orthoclase from a 4-m-wide pod of coarse-grained syenite, and sanidine from a fused ash-flow tuff within 1 m of the lower contact with a large lopolith. For the two ash-flow tuff sanidine separates, step-heating apparent ages increase progressively with the amount of gas released. The minimum ages are 8.65 (±0.10) and 8.66 (±0.18) Ma (all uncertainties are 2σ). We interpret these dates to be maximum estimates of the age of partial outgassing because each age spectrum dropped until the trapped components clouded the signal. An Arrhenius plot for the sanidine data indicates that there were no distinct small domains, which would result in a well-resolved low-temperature plateau. The orthoclase separate from the syenite pod gave an integrated step-heating date of 8.59 ± 0.07 Ma. The age spectrum data do not define a plateau; the integrated age is based on steps 2 to 14 of the age spectrum, with 12 of the 13 dates in this range falling within the uncertainty.
38. S. C. Cande and D. V. Kent [*J. Geophys. Res.* **97**, 13917 (1992)] give the age of chron C4An as 8.861 to 8.529 Ma.
39. W. B. Harland, A. V. Cox, P. G. Llewellyn, A. G. Smith, R. Walters [*A Geologic Time Scale 1989* (Cambridge Univ. Press, Cambridge, 1990, p. 148)] give the age of chron C4Ar-1 as 8.36 to 8.42 Ma and that of chron C4Ar-2 as 8.66 to 8.71 Ma.
40. For example, at site 43 (results not included in Fig. 3), all samples of remagnetized ash-flow tuffs collected within 2 m of a vertical mafic dike have natural remanent magnetization directions of about *D* = 230°, *I* = −5°. With demagnetization, magnetizations carried by magnetite define great circle trajectories, with over 50° of arc, to values of about *D* = 290°, *I* = +35°.
41. D. Gubbins and G. Sarson, *Nature* **368**, 51 (1994).
42. G. A. Valentine, B. M. Crowe, F. V. Perry, *Am. Nucl. Soc. Proc. High-Level Rad. Waste Manage. Conf.* **2**, 2344 (1992).
43. Models incorporating more complex, convective cooling behavior give higher cooling rates and therefore shorter time periods for magnetization blocking.
44. C. A. Wood, *J. Volcanol. Geotherm. Res.* **8**, 315 (1980).
45. F. M. Byers Jr. and H. Barnes, *U.S. Geol. Surv. Map GQ 552* (1967).
46. Research supported in part by the Yucca Mountain Project Office as part of the Civilian Radioactive Waste Management Program. Additional support provided by the Student Research Allocations Committee and the Department of Earth and Planetary Sciences at the University of New Mexico and by the Geological Society of America. We thank C. Hunt and J. Marvin for assistance with hysteresis measurements.

19 May 1994; received 26 August 1994

Marked Post–18th Century Environmental Change in High-Arctic Ecosystems

Marianne S. V. Douglas,*† John P. Smol, Weston Blake Jr.

Paleolimnological data from three high-arctic ponds on Cape Herschel, Ellesmere Island, Canada, show that diatom assemblages were relatively stable over the last few millennia but then experienced unparalleled changes beginning in the 19th century. The environmental factors causing these assemblage shifts may be related to recent climatic warming. Regardless of the cause, the biota of these isolated and seemingly pristine ponds have changed dramatically in the recent past and any hopes of cataloging natural assemblages may already be fruitless.

Anthropogenic impacts such as acid haze (*1*), acid snow (*2*), and other pollutants (*3*, *4*) continue to encroach on the high Arctic, and the effects of global changes, such as the predicted greenhouse warming, are expected to be amplified in polar regions (*5*). Because of the absence of long-term monitoring data, it is not directly possible to determine background variability or to track the trajectories of past environmental changes.

In consideration of the paucity of long-term monitoring data for the Arctic (*6*), indirect proxy methods must be used to infer past environmental conditions. The abundance of lakes and ponds in high-arctic regions makes paleolimnological approaches powerful tools to assist interpretations of environmental change (*7*). In this report, we analyze diatom assemblages preserved in high-arctic sediments to document pond ontogeny in this extreme environment.

Diatoms are the most widely used group of biological indicators in paleolimnological research, and they are rapidly becoming a primary indicator group for several large-scale and long-term biomonitoring programs of environmental change (*8*). Diatoms are abundant, ecologically diverse, and are known to respond, in a quantifiable manner, to environmental changes. Moreover, the siliceous cell walls (frustules) of diatoms are usually well preserved in lake and pond sediments.

Ellesmere Island is the northernmost island in the Canadian Arctic archipelago (Fig. 1). Cape Herschel (78°37'N, 74°42'W), located on the east-central coast of the island facing Smith Sound, is a rugged peninsula (about 2 km by 5 km) of high relief (0 to 285 m above sea level) composed of granitic bedrock overlain by small patches of calcareous till (*9*). No glaciers now occupy the cape, but small patches of snow persist throughout the summer, and glaciers are present to the immediate north and south. As in other high-arctic locations, vegetation is scant, consisting mainly of mosses, grasses,

---

M. S. V. Douglas and J. P. Smol, Paleoecological Environmental Assessment and Research Laboratory, Department of Biology, Queen's University, Kingston, Ontario K7L 3N6, Canada.
W. Blake Jr., Geological Survey of Canada, 601 Booth Street, Ottawa, Ontario, K1A 0E8, Canada.

*To whom correspondence should be addressed.
†Present address: Department of Geology and Geography, University of Massachusetts, Amherst, MA 01003, USA.

sedges, *Salix*, and a few additional flowering plants (*10*).

Cape Herschel is characterized by an abundance of ponds, 36 of which have been monitored for 4 years (*11–17*). The ponds are typically shallow (<2 m), clear, oligotrophic, and freshwater. Thaw typically begins in June, and freeze-up may begin in early August. Elison Lake, Camp Pond, and Col Pond were chosen for detailed study (all names are unofficial except for Elison). These sites represent a spectrum of pond types that includes the largest (Elison) and one of the smallest (Camp) ponds on the cape, and one of low elevation (Elison, at 13 m above sea level) as well as one of the highest sites (Col, at 135 m above sea level).

Frozen pond sediment cores were collected with a SIPRE (CRREL) corer (*18–20*) and kept frozen until they were sectioned into increments of 0.5 or 1 cm. Diatom microfossil analyses followed standard procedures; species lists, other ecological and taxonomic information, and methodologies are detailed elsewhere (*12*). Biogenic silica analyses (*21*) were used to estimate past diatom production (*12*). We obtained ^{14}C dates for the basal sediments and used ^{210}Pb dating for the recent sediments. The ^{14}C dates indicate that the Elison Lake core covers 3850 ± 100 years (GSC-3170) or 4417 to 4140 calibrated years; the Camp Pond core covers 5760 ± 100 years (GSC-2990) or 6727 to 6452 calibrated years; and the Col Pond core covers at least 8000 years (*22*) of sediment accumulation. Contiguous ^{210}Pb dating of the recent sediments (Fig. 2) indicates that the entire unsupported ^{210}Pb inventory is contained in the upper 3 cm of the Elison Lake and Camp Pond cores and the top 4 cm of the Col Pond core, indicating an approximate date of 1850 A.D. Such low sedimentation rates are typical of arctic regions.

Several independent lines of evidence (*12*) clearly demonstrate that the pond sediments have not been significantly disturbed. For example, it would not be possible to record such striking successional changes in the diatom record, nor would we obtain such clear ^{210}Pb profiles (Fig. 2), if the sediment cores were mixed.

The diatom assemblage of Elison Lake was dominated by the pioneering *Fragilaria construens/pinnata* complex, having only small proportions of other taxa, throughout all but the lake's most recent history (Fig. 2A). The amount of the moss epiphyte *Pinnularia balfouriana*, which represented about 10% of the assemblage throughout the core, increases dramatically in the post–18th century sediments, where it eventually comprised close to 90% of the diatom assemblage.

As with Elison Lake, Col Pond's diatom flora was dominated by small benthic *Fragilaria* spp. until the 19th century, where there is a complete floristic shift to a relatively diverse assemblage of *Achnanthes*, *Caloneis*, *Cymbella*, *Navicula*, *Nitzschia*, and *Kraskella* taxa (Fig. 2C). A second, replicate core contained virtually identical species shifts (*12*).

Camp Pond's development is dominated by *Denticula kuetzingii*, *F. pinnata*, *Nitzschia frustulum*, and other *Nitzschia* spp. (Fig. 2B). The species *F. pinnata* undergoes an interesting successional pattern, in that it dominated the pond's early development, then waned in relative abundance near a depth of 80 cm, then increased again near a depth of 20 cm, only to virtually disappear in the surface sediments (Fig. 2B). The pond's recent sediments are characterized by dramatic increases in the relative frequencies of *Achnanthes* spp.

Diatom assemblages have clearly changed in the ponds' histories; the most striking shifts began in the 19th century and continue to the present time. Relatively few changes appear to have occurred before the 19th century, and those that did likely reflect subtle, long-term limnological or environmental changes that occurred on Cape Herschel. Not surprisingly, the smallest pond (Camp) shows the greatest variability in the pre–19th century successions. Nonetheless, these changes are dwarfed by the more recent assemblage shifts where new taxa dominate.

The causes of the post–18th century diatom shifts are uncertain. We had originally assumed that the 36-pond surface-sediment diatom calibration set from Cape Herschel (*13*), which was augmented by present-day periphyton data (*17*), would assist these interpretations. However, as was evident within a few centimeters below the sediment-water interface of the cores, the pond environments have changed so substantially over the last two centuries that analogs no longer exist on the cape for the pre–19th century pond assemblages. Immigration of new taxa into the area is not a possible cause for the recent floristic changes because the diatoms that dominate the recent sediments were always present in the ponds, albeit usually at trace levels.

The recent floristic changes, which are unprecedented in the ponds' histories, occurred mainly in the 19th century, the period of potential anthropogenic impact. This impact could not be of a local nature, as the

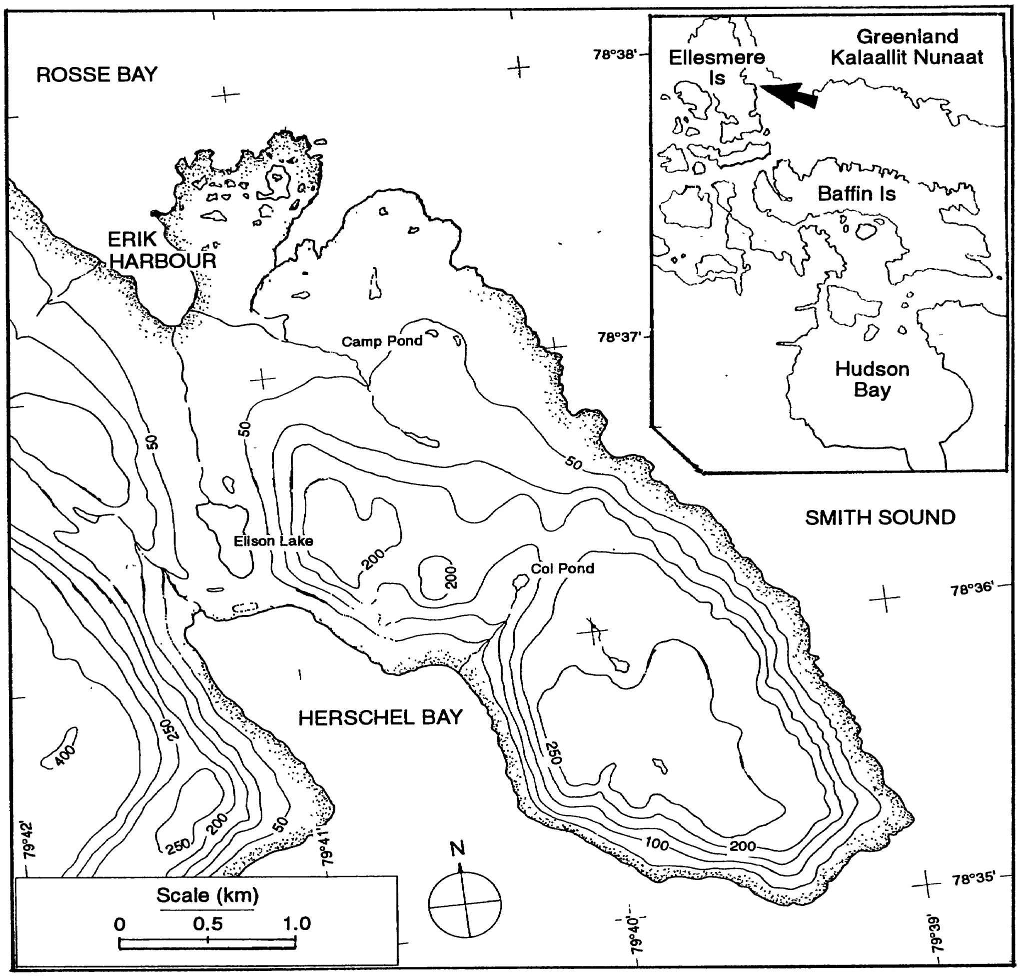

Fig. 1. Location map showing Cape Herschel and the three study ponds. Elevations are in meters above sea level.

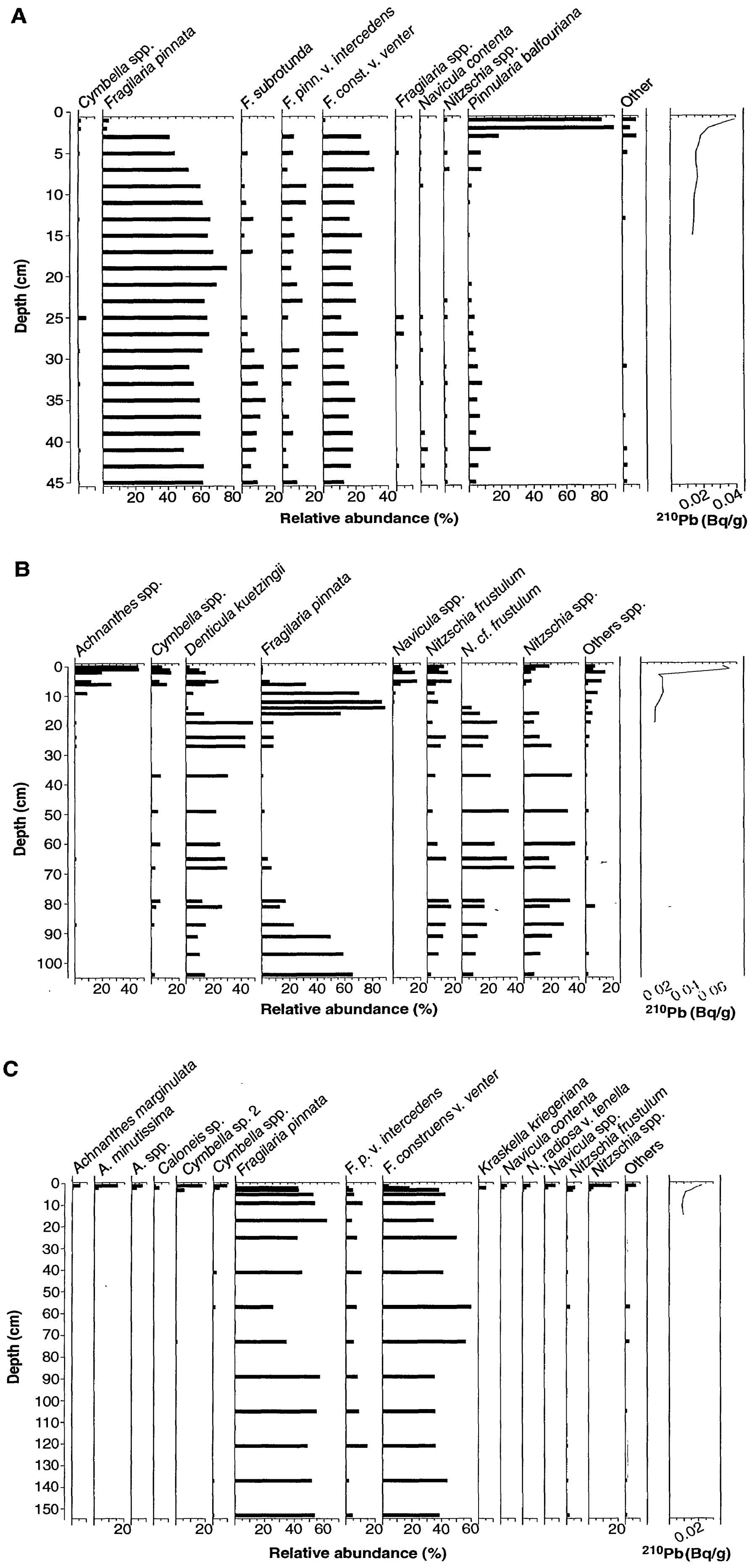

Fig. 2. Relative frequency diagrams of the dominant diatom taxa recorded in the Cape Herschel pond sediments. (**A**) Elison Lake, (**B**) Camp Pond, and (**C**) Col Pond. The ^{210}Pb activity in becquerels (Bq) per gram is shown at the right.

Cape Herschel peninsula was never inhabited, except for some Inuit hunting parties for short stays in camps near the sea, but this occurred at intervals over the last 3500 years (*23*).

Airborne pollution, transported long distances, may be affecting the ponds, and trace levels of some pollutants have been detected on Cape Herschel (*3*). The diatom changes, however, predate the deposition of these contaminants. Moreover, Pb-isotope analyses of the pond sediments do not indicate any anthropogenic-related Pb deposition in these ponds (*24*). Although the area may be receiving some acidic deposition, the ponds are still well buffered and alkaline (pH $\approx$8.5).

Areas such as Cape Herschel currently receive higher doses of ultraviolet (UV) radiation than in the past, which may affect algal assemblages (*25*). Changes in UV radiation, however, are believed to be recent and had not begun to increase as long as 200 years ago.

An alternative hypothesis is recent climatic warming. If climate ameliorated even slightly, it would have had a dramatic effect on the diatom assemblages. We previously speculated (*11*, *13*) on how the diatom community at Cape Herschel would respond to climatic warming, and indeed, the diatom changes recorded in the post–18th century sediments are in agreement with these predictions. For example, with even slight warming, the length of the growing season would be significantly longer, thus allowing for the development of more diverse and complex diatom communities. This development has happened in all the study ponds. Submerged mosses would also be more abundant, and arctic moss epiphytes (*12*) indeed increase in relative frequencies [for example, the arctic moss epiphyte *P. balfouriana* increases dramatically in the top 3 cm of Elison Lake (Fig. 2A)]. Meanwhile, benthic *Fragilaria* spp. still dominate nearby deep, cold, ice-covered lakes (*7*).

Although species composition has been greatly altered, biogenic silica analyses (*12*) show that overall diatom abundance has not changed markedly. As shown in other regions where diatoms have been used for environmental assessments (*8*), species assemblage data are the most sensitive monitors of environmental change in these ponds.

Ponds are ubiquitous features of much of the Arctic. Because of their small volumes, they may be especially sensitive bellwethers of environmental change. Our data indicate that unprecedented environmental changes, most likely related to climatic warming, have occurred since the beginning of the 19th century. Other workers, using different proxy methods, have also indicated recent climatic warming in different arctic regions (*26*, *27*), but our data indicate an earlier (by over a century) start for these changes.

Given the absence of comparable paleolimnological studies from other high-latitude ponds, we cannot yet determine how widespread these changes have been. Any attempts at cataloging pristine arctic assemblages may already be too late, as our data indicate that high-arctic ponds have already changed.

REFERENCES AND NOTES

1. R. A. Kerr, *Science* **212**, 1013 (1981).
2. R. M. Koerner and D. Fisher, *Nature* **295**, 137 (1982).
3. R. McNeely and W. D. Gummer, *Arctic* **37**, 210 (1984).
4. L. A. Barrie *et al.*, *Sci. Total Environ.* **122**, 1 (1992).
5. J. T. Houghton, G. J. Jenkins, J. J. Ephraums, Eds., *Climate Change: The IPCC Scientific Assessment* (Cambridge Univ. Press, Cambridge, 1990).
6. D. W. Gullet and W. R. Skinner, *The State of Canada's Climate: Temperature Change in Canada 1859-1991* (State of the Environment Rep. 92-2, Atmospheric Environment Service, Environment Canada, Ottawa, 1992).
7. J. P. Smol, *Verh. Int. Verein. Limnol.* **23**, 837 (1988).
8. S. S. Dixit, J. P. Smol, J. C. Kingston, D. F. Charles, *Environ. Sci. Technol.* **26**, 23 (1992).
9. W. Blake Jr., *Geol. Surv. Can. Pap.* **77-1C**, 107 (1977).
10. J. Bridgland and J. M. Gillett, *Can. Field Nat.* **97**, 279 (1983).
11. M. S. V. Douglas, thesis, Queen's University (1989).
12. ______, thesis, Queen's University (1993).
13. ______ and J. P. Smol, *Nova Hedwigia Z. Kryptogamenkd.* **57**, 511 (1993).
14. ______, *Arch. Hydrobiol.*, in press.
15. K. E. Duff, M. S. V. Douglas, J. P. Smol, *Nord. J. Bot.* **12**, 471 (1992).
16. T. Nogrady and J. P. Smol, *Hydrobiologia* **173**, 231 (1989).
17. M. S. V. Douglas and J. P. Smol, *J. Phycol.*, in press.
18. W. Blake Jr., *Geol. Surv. Can. Pap.* **78-IC**, 119 (1978).
19. ______, *ibid.* **82-1C**, 104 (1982).
20. The corer was from a design developed by the Snow, Ice, and Permafrost Research Establishment (SIPRE), now the Cold Regions Research and Engineering Laboratory (CRREL).
21. D. J. Conley, *Biogeochemisty* **6**, 161 (1988).
22. W. Blake Jr., *Can. J. Earth Sci.* **29**, 1958 (1992).
23. P. Schledermann, *Crossroads to Greenland* (Komatik Ser. no. 2, Arctic Institute of North America, University of Calgary, Calgary, 1990).
24. J. Blais, personal communication.
25. S. Roy and W. F. Vincent, *Environ. Rev.* **1**, 1 (1993).
26. R. M. Koerner and D. A. Fisher, *Nature* **343**, 630 (1990).
27. R. S. Bradley, *Quat. Sci. Rev.* **9**, 365 (1990).

28. This research was supported by the Natural Sciences and Engineering Research Council of Canada, Polar Continental Shelf Project, Geological Survey of Canada (contribution 12494), Northern Studies Training Program, and the Cape Herschel Project (contribution 50). The ^{210}Pb dating was performed by B. Risto and R. J. Cornett at the Atomic Energy Canada. This paper benefited from comments by R. Bradley, H. J. Birks, R. Scherer, R. Koerner, J. Bourgeois, B. Cumming, and scientists at the Paleoecological Environmental Assessment and Research Laboratory.

2 June 1994; accepted 31 August 1994

Strength of Diamond

Donald J. Weidner, Yanbin Wang, Michael T. Vaughan

The yield strength of diamond is measured under a pressure of 10 gigapascals at temperatures up to 1550°C by the analysis of x-ray peak shapes on diamond diffraction lines in a powdered sample as a function of pressure and temperature. At room temperature, the diamond crystals exhibit elastic behavior with increasing pressure. Significant ductile deformation is observed only at temperatures above 1000°C at this pressure. The differential yield strength of diamond decreases with temperature from 16 gigapascals at 1100°C to 4 gigapascals at 1550°C. Transmission electron microscopy observations on the recovered sample indicate that the dominant deformation mechanism under high pressure and temperature is crystal plasticity.

Diamonds are widely used as indentors as well as cutting, drilling, grinding, and wire-drawing tools that are generally used under high-stress conditions. Diamond anvil cells and large-volume, multianvil apparatus that use polycrystalline diamond compacts are the major instruments for high-pressure–high-temperature research (*1–3*). All of these applications require a knowledge of the strength of diamonds. However, quantitative data for diamond yield strength remain elusive because diamond is so difficult to deform. To measure yield strength, it is generally necessary to apply a force until the material flows, measuring the force and the resulting deformation while separating the effects of fracture from ductile flow. To do this, the deforming apparatus needs to be stronger than the sample; because diamond is the strongest known material, these measurements have been very difficult to accomplish. Therefore, most of the previous strength measurements for diamond have been conducted with indentation (*4*), torsion (*5*), and bending (*6*) techniques. The conversion of these measurements to compressional and tensile strength values is often ambiguous. The heating of diamond at room pressure in excess of 1500°C generally results in extensive graphitization (*7*). Furthermore, ductile deformation in most materials only occurs under sufficient pressures, temperatures, or both (*8*). To determine the ductile deformation of diamond, it is necessary to make the measurements at high temperature and at a pressure within the diamond stability field so that neither brittle failure nor graphitization contributes to the results.

Here we report results on the yield strength of a powdered diamond sample at temperatures up to 1550°C and at a pressure of 10 GPa, conditions that serve both to stabilize the diamond phase of carbon and to provide the driving force to produce deviatoric stresses at grain contacts (*9*). The experiment was conducted with a DIA-type, cubic-anvil, high-pressure apparatus, SAM-85 (*10*). A powdered diamond-polishing compound (Crystallite Corporation, Marina del Ray, California) with an average grain size of 3 μm fills a portion of the sample volume about 0.5 mm long and 1.2 mm in diameter, and powdered NaCl mixed with BN is loaded into the remaining portion of the sample volume. The equation of state of NaCl is used to determine the cell pressure at various temperatures (*11*).

Energy-dispersive x-ray diffraction data are collected at a fixed scattering angle of 10° at the superconducting wiggler beam line (X17B1) at the National Synchrotron Light Source. The x-ray beam is collimated to 100 μm in its vertical dimension and 200 μm in its horizontal dimension. Diffraction spectra of the diamond are collected at the same position in the sample at various temperatures in an energy range up to 100 keV, with a collection time of 300 s. Estimated temperature variation in the diffracting volume is less than 5°C (*12*).

We use the method described in (*9*) to obtain information of stress in the sample from diffraction signals. Under a hydrostatic pressure boundary condition, heterogeneities within the sample along with elastic anisotropy are responsible for generating stresses that vary from grain to grain. The effect of this microscopic deviatoric stress field is the broadening of x-ray diffraction lines, and the amount of line broadening is an indicator of the distribution of longitudinal strain parallel to the diffraction vector (*13*). The width of the diffraction lines is a convolution of the instrument response, sample response function, and the longitudinal elastic strain distribution parallel to the diffraction vector. Using the room pressure and temperature spectra as a reference for zero strain, we calculate the strain distribution in the sample at elevated pressure and temperature as the root-mean-square broadening. By multiplying the strain by an appropriate aggregate elastic modulus [in the experiment we used

---

Center for High Pressure Research and Department of Earth and Space Sciences, State University of New York, Stony Brook, NY 11794–2100, USA.